Suitable synthetic procedures have now been developed, and the precise identity of the products has been shown to be very dependent on both the S:V and edt^{2-}:V reaction ratios. Such considerations will be important as this work is extended to other thiolate groups. Further studies in this rich new area of early-transition-metal sulfide chemistry are in progress.[37]

Acknowledgment. This work was supported by NSF Grant CHE 8507748. We thank the Bloomington Academic Computing Service for a gift of computer time and Scott Horn for skilled technical assistance.

(37) For the structure of $[V_4S_2(edt)_6]^{2-}$, see: Money, J. K.; Huffman, J. C.; Christou, G. *J. Am. Chem. Soc.* **1987**, *109*, 2210.

Registry No. **1**, 87495-20-3; **2**, 112113-65-2; **3**, 112113-66-3; **4**, 104693-61-0; **5**, 104693-59-6; Na_2edt, 23851-16-3; $(NEt_4)_2[V_2(edt)_4]$, 87145-62-8; $[V_2(edt)_4]^-$, 112113-69-6; $[V_2(edt)_4]$, 112113-70-9; $(NEt_4)_3[V_3S_4(edt)_3]$, 112113-68-5; $[V_3S_4(edt)_3]^{4-}$, 112113-71-0; $[V_3S_4(edt)_3]^{2-}$, 112113-72-1; $[V_3S_4(edt)_3]^-$, 112113-73-2; $[V_2OS_4(edt)]^{4-}$, 112113-74-3; $[V_2S_5(edt)]^{4-}$, 112113-75-4; VCl_3, 7718-98-1; S, 7704-34-9.

Supplementary Material Available: Tables S1-S12, giving fractional coordinates, isotropic and anisotropic thermal parameters, and bond distances and angles for complexes **1**, **2**, and **4** (27 pages); complete listings of observed and calculated structure factors (54 pages). Ordering information is given on any current masthead page. Complete MSC structure reports (No. 83073, 86154, and 85160 for **1**, **2**, and **4**, respectively) are available on request from the Indiana University Chemistry Library.

Contribution from the Department of Chemistry,
The University of North Carolina, Chapel Hill, North Carolina 27514

Redox Properties of Aqua Complexes of Ruthenium(II) Containing the Tridentate Ligands 2,2′:6′,2″-Terpyridine and Tris(1-pyrazolyl)methane

Antoni Llobet,[1a] Pascal Doppelt,[1b] and Thomas J. Meyer*

Received May 27, 1987

A series of complexes containing either the facial tridentate ligand tris(1-pyrazolyl)methane (tpm) ($[(tpm)(b)RuX]^{n+}$ (b = 2,2′-bipyridine (bpy), 4,4′-dimethyl-2,2′-bipyridine (4,4′-$(CH_3)_2$-bpy), 1,10-phenanthroline (phen); X = Cl^-, H_2O, O^{2-})) or the meridional tridentate ligand 2,2′:6′,2″-terpyridine (trpy) (*cis*- and *trans*-$[(trpy)(pic)RuX]^{m+}$ (pic = picolinate anion; X = Cl^-, H_2O, O^{2-})) and the μ-oxo ions *cis*- and *trans*-$[[(trpy)(pic)Ru]_2O]^{2+}$ have all been prepared and their redox properties investigated. As observed in related complexes, *cis*- and *trans*-$[(trpy)(pic)Ru(H_2O)]^+$ and the series $[(tpm)(b)Ru(H_2O)]^{2+}$ undergo two pH-dependent, chemically reversible one-electron oxidations corresponding to the associated Ru(IV)/Ru(III) and Ru(III)/Ru(II) couples. In acetonitrile, the μ-oxo ions *cis*- and *trans*-$[[(trpy)(pic)Ru^{III}]_2O]^{2+}$ undergo reversible one-electron oxidations and reductions while in water a two-electron, pH-dependent, chemically reversible reduction occurs for which the resulting II,II ion appears to be stabilized by formation of a μ-hydroxo bridge.

Introduction

There is by now an extensive higher oxidation state chemistry of Os and Ru based on polypyridyl containing complexes.[2] The higher oxidation states can be reached from the corresponding aqua complexes of Ru(II) or Os(II) by sequential oxidation and proton loss, e.g., eq 1,[2a,b] where bpy is 2,2′-bipyridine and py is

$$(bpy)_2(py)Ru^{II}(H_2O)^{2+} \underset{+1e^-,\,+1H^+}{\overset{-1e^-,\,-1H^+}{\rightleftharpoons}} (bpy)_2(py)Ru^{III}(OH)^{2+} \underset{+1e^-,\,+1H^+}{\overset{-1e^-,\,-1H^+}{\rightleftharpoons}} (bpy)_2(py)Ru^{IV}(O)^{2+} \quad (1)$$

pyridine. The higher oxidation states have an extensive stoichiometric and catalytic chemistry as oxidants.[3] One of the features of interest in this chemistry for us has been that in contrast to more conventional oxidants like MnO_4^- or CrO_3, it is possible, at least in principle, to create a *family* of related oxidants where the redox characteristics can be varied systematically by changing the ligands.

Progress has been made in the design of new oxidatively stable ligand systems that are capable of supporting the higher oxidation states of Ru and Os, most notably by Che and co-workers.[4] We report here on the redox properties of a series of polypyridyl

(1) (a) Fulbright "La Caixa" fellow, Barcelona, Spain. (b) Permanent address: Institut Le Bel, Université Louis Pasteur, 67070 Strasbourg Cedex, France.

(2) (a) Moyer, B. A.; Meyer, T. J. *J. Am. Chem. Soc.* **1978**, *100*, 3601. (b) Moyer, B. A.; Meyer T. J. *Inorg. Chem.* **1981**, *20*, 436. (c) Takeuchi, K. J.; Samuels, G. J.; Gersten, S. W.; Gilbert, J. A.; Meyer, T. J. *Inorg. Chem.* **1983**, *22*, 1407. (d) Pipes, D. W.; Meyer, T. J. *J. Am. Chem. Soc.* **1984**, *106*, 7653. (e) Gilbert, J. A.; Eggleston, D. S.; Murphy, W. R.; Geselowitz, D. A.; Gersten, S. W.; Hodgson, D. J.; Meyer, T. J. *J. Am. Chem. Soc.* **1985**, *107*, 3855. (f) Gilbert, J. A.; Geselowitz, D. A.; Meyer, T. J. *J. Am. Chem. Soc.* **1986**, *108*, 1493. (g) Dobson, J. C.; Takeuchi, K. J.; Pipes, D. W.; Geselowitz, D. A.; Meyer, T. J. *Inorg. Chem.* **1986**, *25*, 2357. (h) Marmion, M. E.; Takeuchi, K. J. *J. Am. Chem. Soc.* **1986**, *108*, 510. (i) Wong, K.-Y.; Che, C.-M.; Anson, F. C. *Inorg. Chem.* **1987**, *26*, 737. (j) Che, C.-M.; Lai, T.-F.; Wong, K.-W. *Inorg. Chem.* **1987**, *26*, 2289.

(3) (a) Moyer, B. A.; Meyer, T. J. *J. Am. Chem. Soc.* **1979**, *101*, 1326. (b) Moyer, B. A.; Thomson, M. S.; Meyer, T. J. *J. Am. Chem. Soc.* **1980**, *102*, 2310. (c) Moyer, B. A.; Sipe, B. K.; Meyer, T. J. *Inorg. Chem.* **1981**, *20*, 1475. (d) Thompson, M. S.; Meyer, T. J. *J. Am. Chem. Soc.* **1982**, *104*, 4106. (e) Thompson, M. S.; Meyer, T. J. *J. Am. Chem. Soc.* **1982**, *104*, 5070. (f) Takeuchi, K. J.; Samuels, G. J.; Gersten, S. W.; Gilbert, J. A.; Meyer, T. J. *Inorg. Chem.* **1983**, *22*, 1409. (g) Thompson, M. S.; De Giovani, W. F.; Moyer, B. A.; Meyer, T. J. *J. Org. Chem.* **1984**, *49*, 4972. (h) Meyer, T. J. *J. Electrochem. Soc.* **1984**, *131*, 221C. (i) Takeuchi, K. J.; Thomson, M. S.; Pipes, D. W.; Meyer, T. J. *Inorg. Chem.* **1984**, *23*, 1845. (j) Dobson, J. C.; Seok, W. K.; Meyer, T. J. *Inorg. Chem.* **1986**, *25*, 1514. (k) Roecker, L.; Meyer, T. J. *J. Am. Chem. Soc.* **1986**, *108*, 4066. (l) Roecker, L.; Dobson, J. C.; Vining, W. J.; Meyer, T. J. *Inorg. Chem.* **1987**, *26*, 779. (m) Roecker, L.; Meyer, T. J. *J. Am. Chem. Soc.* **1987**, *109*, 746.

(4) (a) Che, C.-M.; Tang, T. W.; Poon, C. K. *J. Chem. Soc., Chem. Commun.* **1984**, 641. (b) Che, C.-M.; Wong, K.-Y.; Mak, T. C. W. *J. Chem. Soc., Chem. Commun.* **1985**, 546. (c) Mak, T. C. W.; Che, C.-M.; Wong, K.-Y. *J. Chem. Soc., Chem. Commun.* **1985**, 986. (d) Che, C.-M.; Cheng, W.-K.; Mak, T. C. W. *J. Chem. Soc., Chem. Commun.* **1986**, 200. (e) Che, C.-M.; Wong, K.-Y. *J. Chem. Soc., Chem. Commun.* **1986**, 229. (f) Che, C.-M.; Wong, K.-Y.; Leung, W.-H.; Poon, C. K. *Inorg. Chem.* **1986**, *25*, 345. (g) Che, C.-M.; Yam, V. W.-W. *J. Am. Chem. Soc.* **1987**, *109*, 1262.

0020-1669/88/1327-0514$01.50/0

complexes of Ru based on two tridentate ligands. The first is 2,2′:6′,2″-terpyridine (trpy), which given the structural constraints

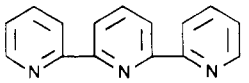

trpy

of the ligand, must adopt the meridional geometry illustrated in the following structure where the trpy ligand is represented as arc-connected N atoms.

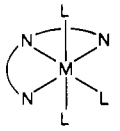

The second tridentate ligand is tris(1-pyrazolyl)methane (tpm),

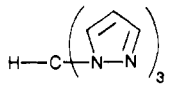

tpm

which by its structure and the established structural chemistry of the related hydroxy derivative, tris(1-pyridyl)methanol[5] is constrained to assume the facial geometry

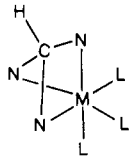

Experimental Section

Materials. All reagents were ACS grade and were used without further purification. Elemental analyses were performed by Galbraith Laboratories, Knoxville TN.

Preparations. [(trpy)$RuCl_3$] was prepared as previously described.[6]

***cis*- and *trans*-[(trpy)(pic)RuCl]·H_2O.** A 0.50-g quantity of [(trpy)-$RuCl_3$] and 0.14 g of picolinic acid were heated at reflux for 3 h in 100 mL of absolute ethanol containing 0.5 g of LiCl and 0.5 mL of triethylamine. The pot content was cooled to room temperature and the

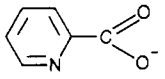

picolinate anion, pic

volume reduced to 30 mL with a rotary evaporator. Distilled water (30 mL) was added, the volume again reduced to 30 mL, and the pot content chilled overnight in a refrigerator. The dark brown solid was collected on a frit, washed with water (5 × 20 mL) and air dried. Purification was achieved by column chromatography (3 × 10 cm) using alumina as the column support and acetonitrile as the eluant. Under these conditions, the trans isomer was eluted leaving the cis isomer on the column. The cis isomer was extracted from the column by using an ethanol–acetonitrile (1:4) mixture. For the cis isomer: yield 90 mg, 15.5%. Anal. Calcd for $C_{21}H_{17}ClN_4O_3Ru$: C, 49.4; H, 3.3; N, 11.0. Found: C, 49.6; H, 3.2; N, 11.2. For the trans isomer: yield 240 mg, 41.4%. Anal. Found: C, 48.0; H, 3.3; N, 11.7.

***cis*- and *trans*-[(trpy)(pic)Ru(H_2O)](ClO_4).** A 0.1-g quantity of *cis*- or *trans*-[(trpy)(pic)RuCl]·H_2O and 0.092 g of $AgClO_4$·H_2O (2 equiv) were heated together at reflux under argon for 2 h in 60 mL of acetone–water (3:1). AgCl was filtered off, the solution volume was reduced to 15 mL, and separation of the components was achieved by column chromatography (1 × 3 cm) using Bio-Rex 70 (400 mesh, sodium form) as the column support. An orange-brown band was obtained by using 0.02 M $NaClO_4$ as the eluant. The eluted band was reduced in volume by rotary evaporation until a precipitate began to form. The solution was chilled overnight at 5 °C, and the black product was recovered by filtration, washed twice with 1 mL of cold distilled water, and air dried. Yield: 65 mg, 62%. Anal. Calcd for $C_{21}H_{17}ClN_4O_7Ru$: C, 43.9; H, 2.9; N, 9.8. Found for the cis isomer: C, 44.2; H, 3.1; N, 10.1. Found for the trans isomer: C, 44.0; H, 3.1; N, 9.9.

***cis*- or *trans*-[[(trpy)(pic)Ru]$_2$O](ClO_4)$_2$·$4H_2O$.** A 0.2-g amount of *cis*- or *trans*-[(trpy)(pic)RuCl]·H_2O and 0.18 g of $AgClO_4$·H_2O (2 equiv) were heated together at reflux for 3 h in 50 mL of water. AgCl was filtered off. The purification of the blue-green compound was carried out by using the same method described for the aqua monomers but with a 0.1 M $NaClO_4$ solution as eluant. Crystals of the dimer appeared by slow evaporation of the solution recovered from the column. Yield: 137 mg, 60.0%. Anal. Calcd for $C_{42}H_{34}Cl_2N_8O_{15}Ru_2$: C, 42.0; H, 3.0; N, 9.3. Found for the cis isomer: C, 42.5; H, 3.0; N, 9.4. Found for the trans isomer: C, 42.0, H, 3.3; N, 9.3.

***trans*-[(trpy)(pic)Ru(O)](ClO_4)·$2H_2O$.** A 50-mg amount of *trans*-[(trpy)(pic)Ru(H_2O)](ClO_4) was dissolved in 50 mL of distilled water containing 2 mL of saturated LiCl in water. The solution was cooled to 0 °C and a drop of liquid bromine added. The light orange precipitate that formed was collected on a frit, washed twice with a minimum of cold water, and air dried. Yield: 30 mg, 56%. Anal. Calcd for $C_{21}H_{19}ClN_4O_9Ru$: C, 41.4; H, 3.1; N, 9.2. Found: C, 41.8; H, 2.8; N, 9.2.

Tris(1-pyrazolyl)methane (tpm). The ligand was prepared by a modified method of Huckel and Bretschneider.[7]

[(tpm)$RuCl_3$]·$1.5H_2O$. A 1.00 g amount of $RuCl_3$·xH_2O and 0.82 g of tpm were heated at reflux for 4 h in 350 mL of absolute ethanol. The greenish brown solid was filtered in a Buchner funnel, washed with absolute ethanol (3 × 30 mL) and acetone (3 × 30 mL) and air dried. Yield: 1.21 g, 70.4%. Anal. Calcd for $C_{10}H_{13}Cl_3N_6O_{1.5}Ru$: C, 26.75; H, 2.90; N, 18.72. Found: C, 26.89; H, 3.02; N, 18.36.

[(tpm)(bpy)RuCl]Cl·$2H_2O$. A 0.50-g quantity of [(tpm)$RuCl_3$]·$1.5H_2O$ and 0.20 g of bpy were heated at reflux for 5 min in 100 mL of ethanol–water (3:1) containing 0.5 g of LiCl, 12 drops of NEt_3 were added, and the mixture was heated at reflux for an additional 10 min. The brown solution was filtered hot and the volume reduced to 25 mL in a rotary evaporator. The pot content was chilled overnight, and the resulting brown crystals were collected in a Buchner funnel, washed with a minimum amount of cold water, and air dried. Yield: 264 mg, 41%. Anal. Calcd for $C_{20}H_{22}Cl_2N_8O_2Ru$: C, 41.52; H, 3.81; N, 19.38. Found: C, 41.96; H, 3.78; N, 19.50.

[(tpm)(phen)RuCl]Cl·$1.5H_2O$. The same procedure was utilized as in the previous preparation, but the volume was reduced to dryness and the resulting solid recrystallized from hot ethanol. Brown crystals appeared, which were filtered, washed with a minimum amount of cold ethanol, and air dried. Yield: 375 mg, 66.1%. Anal. Calcd for $C_{22}H_{21}Cl_2N_8O_{1.5}Ru$: C, 44.52; H, 3.55; N, 18.80. Found: C, 44.47; H, 4.27; N, 18.20.

[(tpm)(4,4′-$(CH_3)_2$-bpy)RuCl]Cl·$1.5H_2O$. The same procedure was utilized as in the preparation of the bpy complex, but the volume was reduced until a solid began to precipitate. The pot content was chilled in a refrigerator for 4 h, and the resulting brown crystals were filtered, washed with a minimum amount of cold water, and air dried. Yield: 320 mg, 48.1%. Anal. Calcd for $C_{22}H_{25}Cl_2N_8O_{1.5}Ru$: C, 44.21; H, 4.19; N, 18.75. Found: C, 43.94; H, 4.32; N, 18.48.

[(tpm)(b)Ru(H_2O)](ClO_4)$_2$ (b = bpy, phen, 4,4′-$(CH_3)_2$-bpy). In a typical experiment a 0.25-g amount of [(tpm)(bpy)RuCl]Cl·$2H_2O$ and 179 mg of $AgClO_4$·H_2O were heated at reflux for 2 h in 33 mL of acetone–water (3:1). AgCl was filtered off and the volume reduced in a rotary evaporator until an orange crystalline solid began to form. The pot content was chilled in a refrigerator for 4 h, and the resulting crystals were filtered, washed with a small amount of cold water, and air dried. Yield: 260 mg, 87.4%. ^1H NMR (D_2O): δ 8.60 (d, 2, J_{ab} = 5.6 Hz, H_a), 8.43 (d, 2, J_{cd} = 7.8 Hz, H_d), 8.32 (d, 2, $J_{\alpha\beta}$ = 2.7 Hz, H_α), 8.12 (d, 1, $J_{\alpha'\beta'}$ = 2.7 Hz, $H_{\alpha'}$), 8.08 (d, 2, $J_{\beta\gamma}$ = 1.9 Hz, H_γ), 7.92 (double t, 2, J_{bc} = J_{cd} = 7.8 Hz, J_{ac} = 1 Hz, H_c), 7.38 (doublet of doublets, 2, J_{ab} = 5.6 Hz, J_{bd} = 1 Hz, H_b), 6.60 (doublet, 2, $J_{\alpha\beta}$ = 2.7 Hz, $J_{\beta\gamma}$ = 1.9 Hz, H_β), 6.43 (d, 1, $J_{\beta'\gamma'}$ = 1.9 Hz, $H_{\gamma'}$), 6.05 (doublet, 1, $J_{\alpha'\beta'}$ = 2.7 Hz, $H_{\beta'}$). Anal. Calcd for $C_{20}H_{20}Cl_2N_8O_9Ru$: C, 34.88; H, 3.11; N, 16.28. Found: C, 35.05; H, 2.96; N, 16.10. For b = phen: yield 237 mg, 76.1%. Anal. Calcd for $C_{22}H_{23}Cl_2N_8O_{10.5}Ru$: C, 35.72; H, 3.11; N, 15.16. Found: C, 35.74; H, 3.04; N, 14.95. For b = 4,4′-$(CH_3)_2$-bpy: yield 250 mg, 83.4%. ^1H NMR (D_2O): δ 8.45 (d, 2, J_{ab} = 5.6 Hz, H_a), 8.36 (bs, 2, H_α), 8.30 (s, 2, H_d), 8.14 (bs, 1, $H_{\alpha'}$), 8.11 (bs, 2, H_γ), 7.25 (d, 2, J_{ba} = 5.6 Hz, H_b), 6.60 (bs, 2, H_β), 6.45 (bs, 1, $H_{\gamma'}$), 6.09 (bs, 1, $H_{\beta'}$), 2.48 (s, 6, CH_3). Anal. Calcd for $C_{22}H_{24}Cl_2N_8O_9Ru$: C, 36.87; H, 3.35; N, 15.64. Found: C, 36.35; H, 3.40; N, 15.27.

The ^1H NMR assignments are keyed to the structure drawn in Figure 1B.

[(tpm)(bpy)Ru(O)](ClO_4)$_2$·$0.5H_2O$. A 79.5-mg sample of $(NH_4)_2$-$Ce(NO_3)_6$ was dissolved in 5 mL of 2 M $HClO_4$ and this solution was added dropwise to 50.0 mg of [(tmp)(bpy)Ru(H_2O)](ClO_4)$_2$ previously dissolved in 15 mL of warm water. The resulting solution was stirred

(5) Szalda, D. J.; Keene, F. R. *Inorg. Chem.* **1986**, *25*, 2795.
(6) Sullivan, B. P.; Calvert, J. M.; Meyer, T. J. *Inorg. Chem.* **1980**, *19*, 1404.
(7) Huckel, W.; Bretschneider, H. *Ber. Chem.* **1937**, *9*, 2024.

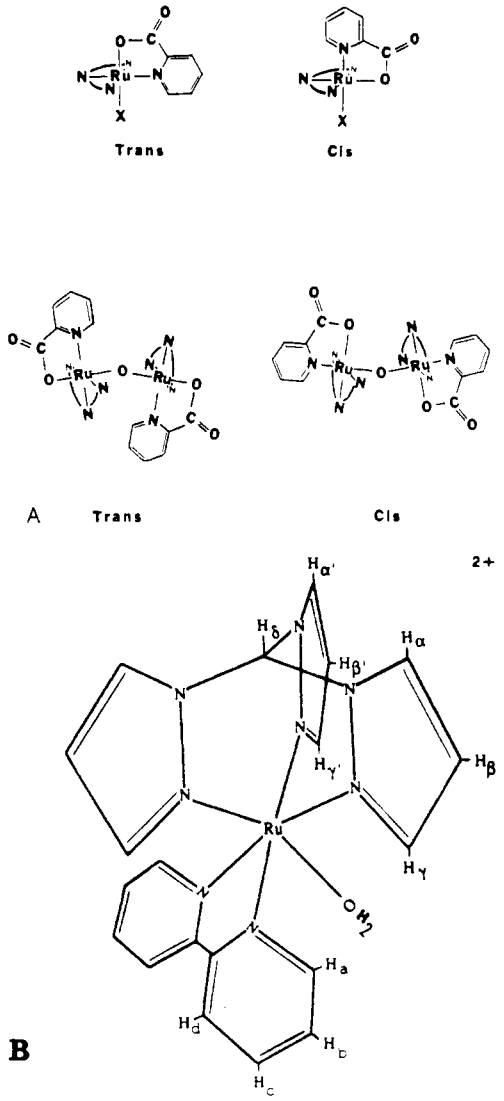

Figure 1. (A) Illustrations of cis and trans isomers in the monomeric and dimeric picolinate derivatives. The trpy ligands are represented as N atoms with connecting arcs. The dimers are assumed to be bent along the Ru–O–Ru axis, a feature that has been established for the related dimers $[(bpy)_2(NO_2)Ru–O–Ru(NO_2)(bpy)_2]^{2+}$[9b] and $[(bpy)_2(H_2O)Ru–O–Ru(H_2O)(bpy)_2]^{4+}$.[2e] (B) Drawn structure of $[(tpm)(bpy)Ru(H_2O)]^{2+}$ illustrating the coordination geometry. The tpm and bpy protons are labeled according to their assignment in the Experimental Section.

for 30 min at room temperature. A green solid appeared, which was filtered, washed with 3 mL of 2 M $HClO_4$ and a small amount of cold water, and air dried. Yield: 30 mg, 59.4%. Anal. Calcd for $C_{20}H_{19}Cl_2N_8O_{9.5}Ru$: C, 34.52; H, 2.73; N, 16.11. Found: C, 34.21; H, 2.78; N, 15.91.

Measurements. Cyclic voltammetric measurements were carried out by using a PAR Model 173 potentiostat/galvanostat or a PAR 264A polarographic analyzer/stripping voltameter. Coulometric measurements were made by using a PAR Model 179 digital Coulometer. The cyclic voltammetric measurements utilized an activated Teflon-sheathed glassy-carbon disk (1.5-mm radius) working electrode,[8] platinum-wire auxiliary electrode, and a saturated sodium chloride calomel reference electrode (SSCE) in a one-compartment cell. The concentration of the complexes was approximately 0.5 mM. The pH was adjusted from 0–2 with trifluoromethanesulfonic acid; sodium trifluoromethanesulfonate was added as electrolyte to keep a minimum ionic strength of 0.1 M. From 2–12 the pH was adjusted with 0.1 M phosphate buffers. Diluted NaOH solutions were used to achieve pH 12–13 with sodium trifluoromethanesulfonate as supporting electrolyte. The pH measurements were made with a Radiometer pHM62 pH meter. All $E_{1/2}$ values reported in this work were estimated from cyclic voltametry as an average of the oxidative and reductive peak potential $(E_{p,a} + E_{p,c})/2$. UV–visible spectra were recorded by using Bausch & Lomb or Hewlett-Packard Model 8451A UV–vis diode-array spectrophotometers with matched quartz 1-cm cells. The ^1H NMR spectra were recorded on an IBM AC-200 spectrometer.

(8) Cabaniss, G. E.; Diamantis, A. A.; Murphy, W. R., Jr.; Linton, R. W.; Meyer, T. J. *J. Am. Chem. Soc.* **1985**, *107*, 1845.

Table I. Electrochemical Data, $E_{1/2}$ (V vs SSCE), in Acetonitrile at 23 °C (μ = 0.1 M Tetraethylammonium Perchlorate)

compound	$E_{1/2}$, V
trans-[(trpy)(pic)RuCl]	0.39
cis-[(trpy)(pic)RuCl]	0.46
trans-$[[(trpy)(pic)Ru]_2O]^{2+}$ [a]	0.75, −0.11, −0.71
cis-$[[(trpy)(pic)Ru]_2O]^{2+}$ [a]	0.73, −0.12, −0.79
$[(tpm)(bpy)RuCl]^+$	0.68
$[(tpm)(phen)RuCl]^+$	0.67
$[(tpm)(4,4'-(CH_3)_2-bpy)RuCl]^+$	0.63

[a] In water at pH 7.0 a single, pH-dependent, 2-electron-reduction wave appears at $E_{1/2}$ = −0.03 V for the cis isomer and 0.09 V for the trans isomer (Figure 2).

Results

Preparation and Characterization of Compounds. Isomerization in the trpy Complexes. The key intermediates in the preparation of both the trpy and the tpm series are the trichlorides [Ru(trpy)Cl_3] and [Ru(tpm)Cl_3]. Subsequent labilization of Cl^- was achieved by reduction to Ru(II) by using NEt_3 as the reducing agent in the presence of the desired ligand.

For the trpy complexes based on the picolinate (pic) ligand, chromatography on alumina reveals the presence of two isomers that are labeled cis and trans with regard to the relative disposition of the pyridyl group on the pic ligand with regard to the central pyridyl group of the 2,2′:6′,2″-terpyridine ligand as illustrated in Figure 1. A tentative assignment of the isomers can be made on the basis of a number of observations: (1) The trans isomer appears to be less polar as shown by its elution characteristics and is the sole product when the reaction is carried out in absolute ethanol. Both isomers are formed in significant amounts in ethanol–water. (2) As found in the related isomeric pairs *cis*- and *trans*-[(trpy)Ru(PPh_3)Cl_2],[6] the trans isomers of [(trpy)(pic)RuCl] and $[(trpy)(pic)Ru(H_2O)]^+$ have lower Ru(III)/Ru(II) potentials (Table II), and for the cis isomer λ_{max} values for the Ru(II) → trpy MLCT absorption bands occur at lower energies, Table III. (3) The stereochemistry is retained upon oxidation. Complexes of Ru(IV) prepared by bromine oxidation

$$Br_2 + [(trpy)(pic)Ru^{II}(H_2O)]^{2+} \rightarrow 2Br^- + 2H^+ + [(trpy)(pic)Ru^{IV}(O)]^{2+} \quad (2)$$

give the same cyclic voltammograms as the corresponding Ru(II) aqua complexes. (4) The stereochemistry is also maintained in the μ-oxo dimers prepared from the corresponding chloro complexes of Ru(II) via

$$[(trpy)(pic)Ru^{II}Cl] + Ag^+ \rightarrow [(trpy)(pic)Ru^{II}(H_2O)]^+ + AgCl \quad (3)$$

$$2[(trpy)(pic)Ru^{II}(H_2O)]^+ - 2e^- \rightarrow 2H^+ + H_2O + [[(trpy)(pic)Ru^{III}]_2O]^{2+} \quad (4)$$

The source of oxidative equivalents in reaction 4 may be either O_2 or ClO_4^-. Reduction of the dimers chemically or electrochemically leads back to the Ru(II)–aqua monomer with the retention of the original stereochemistry.

Electrochemistry and Spectra. Electrochemical data for the non-aqua-containing complexes in acetonitrile are given in Table I. Cyclic voltammograms of the μ-oxo ions in water at pH 6.5 are shown in Figure 2.

As observed earlier for $[[(bpy)_2ClRu]_2O]^{2+}$,[9] in acetonitrile, a chemically reversible 1-electron oxidation of the Ru(III)–Ru(III)

(9) (a) Weaver, T. R.; Meyer, T. J.; Adeyemi, S. A.; Brown, G. M.; Eckberg, R. P.; Hatfield, W. E.; Johnson, E. C.; Murray, R. W.; Untereker, D. *J. Am. Chem. Soc.* **1975**, *97*, 3039. (b) Phelps, D. W.; Kahn, E. M.; Hodgson, D. J. *Inorg. Chem.* **1975**, *14*, 2486.

Table II. Potentials in Water at pH 7 vs SSCE and pK_a Values at 23 °C (μ = 0.1 M)

complexes	$E_{1/2}$, V				$pK_a(H_2O)$	
	IV/II	III/II	IV/III	$\Delta E_{1/2}$(IV/III–III/II), V	Ru^{III}	Ru^{II}
trans-[(trpy)(pic)Ru(H_2O)]$^+$	0.33	0.21	0.45	0.24	2.0	10.0
cis-[(trpy)(pic)Ru(H_2O)]$^+$	0.47	0.38	0.56	0.22	3.7	10.0
[(bpy)$_2$(py)Ru(H_2O)]$^{2+}$ [a]	0.48	0.42	0.53	0.11	0.85	10.8
[(trpy)(bpy)Ru(H_2O)]$^{2+}$ [b]	0.55	0.49	0.62	0.13	1.7	9.7
[(NH_3)$_5$Ru(H_2O)]$^{2+}$ [c]	−0.24	−0.34	−0.14	0.20	4.2	
[(tpm)(bpy)Ru(H_2O)]$^{2+}$	0.55	0.40	0.71	0.31	1.9	10.8
[(tpm)(phen)Ru(H_2O)]$^{2+}$	0.56	0.41	0.71	0.30	1.9	10.7
[(tpm)(4,4′-(CH_3)$_2$-bpy)Ru(H_2O)]$^{2+}$	0.50	0.35	0.66	0.31	1.9	11.0

[a] Reference 2b. [b] Reference 10. [c] Reference 14.

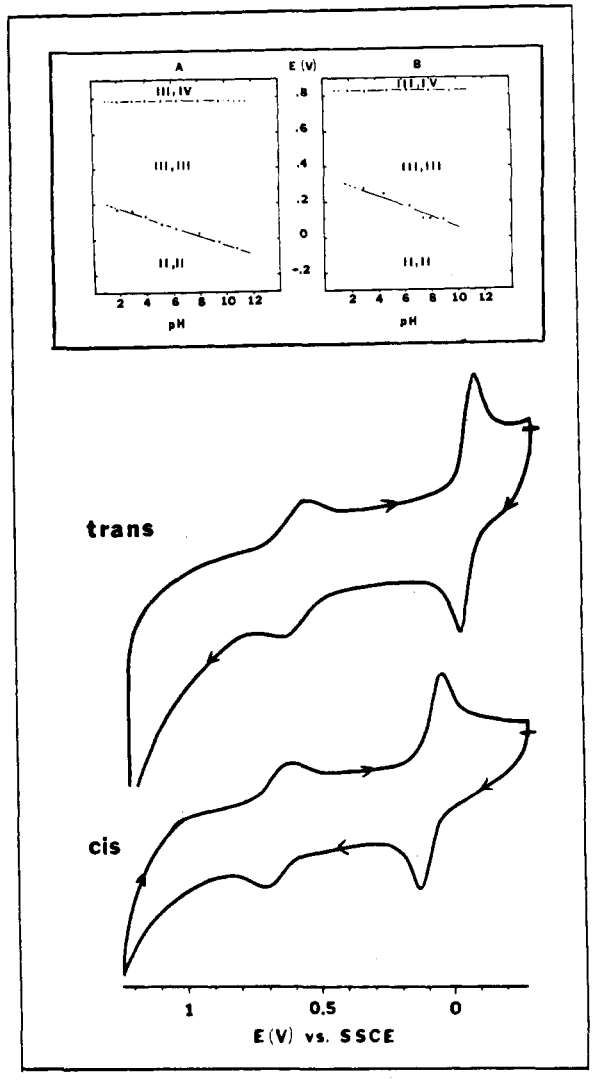

Figure 2. Cyclic voltammograms of *trans*- and *cis*-[[(trpy)(pic)-Ru]$_2$O](ClO$_4$)$_2$ vs SSCE in water at pH 6.5, 0.1M phosphate buffer (scan rate 50 mV/s). The variations of $E_{1/2}$ with pH for the electrochemical processes of both ions are shown in the inset.

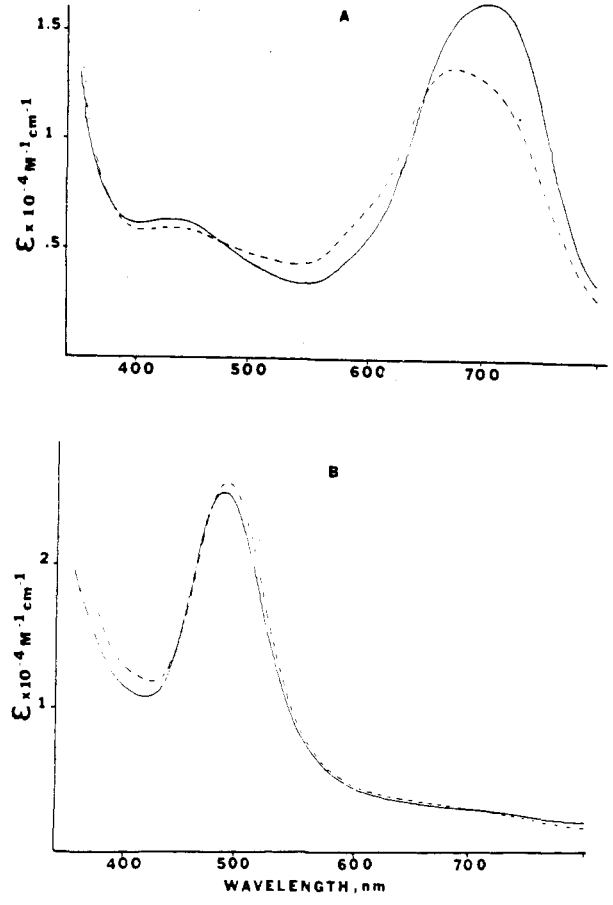

Figure 3. (A) UV–visible spectra of *trans*- (dashed line) and *cis*-[[(trpy)(pic)Ru]$_2$O](ClO$_4$)$_2$ (solid line) in acetonitrile. (B) Spectra after oxidation by an excess of (NH_4)$_2$Ce(NO_3)$_6$.

μ-oxo ions to Ru(III)–Ru(IV) occurs, and a 1-electron reduction to Ru(III)–Ru(II) also occurs, as does a further irreversible reduction that leads to decomposition of the μ-oxo structure with formation of Ru(II). Although the first reduction process is chemically reversible on the cyclic voltametry time scale, attempted coulometry at potentials more negative than the $E_{1/2}$ value for the couple also leads to a net reductive cleavage of the dimer. For the μ-oxo ions the use of oxidation state labels is a convenience. Because of strong electronic coupling across the μ-oxo bridge, a more appropriate description of the Ru(III)–Ru(IV) μ-oxo ion, for example, may be Ru(III.5)–Ru(III.5).

The UV–visible spectra of the Ru(III)–Ru(III) and Ru(II-I)–Ru(IV) forms of the μ-oxo ions, the latter generated in situ by the addition of (NH_4)$_2$Ce^{IV}(NO_3)$_6$, are illustrated in Figure 3, and the UV–visible spectral properties of the series of complexes is summarized in Table III.

In all cases the aqua complexes provide a basis for pH-dependent couples in water with clear evidence found for both Ru(III)/Ru(II) and Ru(IV)/Ru(III) couples. $E_{1/2}$ vs pH or Pourbaix diagrams for the aqua complexes studied are displayed in Figure 5. The drawn diagrams through the experimental points can be generated by using the pK_a values for the Ru(III) and Ru(II) aqua complexes and the $E_{1/2}$ values at pH 7 all of which are collected in Table II. As found earlier for related aqua couples, the cyclic voltammograms for *cis*- and *trans*-[(trpy)(pic)Ru-(H_2O)]$^+$ Ru(IV)/Ru(III) couples (presented as supplementary material) show the effects of slow heterogeneous charge transfer, arising from changes in proton composition between oxidation states.[10]

In water, as in acetonitrile, the III,IV/III,III couple for the cis and trans μ-oxo ions is pH independent but a single, pH-dependent, 2-electron reduction wave is observed. As shown by the insets in Figure 2, the variation with pH is 29 mV/pH unit,

(10) Binstead, R. A.; Meyer, T. J. *J. Am. Chem. Soc.* **1987**, *109*, 3287.

Table III. Visible and Near-UV Absorption Maxima and Extinction Coefficients for Complexes Prepared in This Work

compound	medium	λ_1, nm (log ϵ)	λ_2, nm (log ϵ)
trans-[(trpy)(pic)RuCl]	CH_3CN	550 (3.61)	403 (3.71)
cis-[(trpy)(pic)RuCl]	CH_3CN	519 (3.56)	389 (3.69)
trans-[(trpy)(pic)Ru(H_2O)]$^+$	pH 7	491 (3.81)	
cis-[(trpy)(pic)Ru(H_2O)]$^+$	pH 7	477 (3.80)	
trans-[[(trpy)(pic)Ru^{III}]$_2$O]$^{2+}$	CH_3CN	682 (4.12)	
cis-[[(trpy)(pic)Ru^{III}]$_2$O]$^{2+}$	CH_3CN	698 (4.21)	
trans-[(trpy)(pic)Ru^{III}–O–Ru^{IV}(pic)(trpy)]$^{3+}$ [a]	CH_3CN	480 (4.41)	
cis-[(trpy)(pic)Ru^{III}–O–Ru^{IV}(pic)(trpy)]$^{3+}$ [a]	CH_3CN	479 (4.40)	
[(tpm)(bpy)RuCl]$^+$	CH_3CN	474 (3.54)	346 (3.78)
[(tpm)(phen)RuCl]$^+$	CH_3CN	450 (3.81)	290 (4.09)
[(tpm)(4,4′-$(CH_3)_2$-bpy)RuCl]$^+$	CH_3CN	466 (3.63)	346 (3.93)
[(tpm)(bpy)Ru(H_2O)]$^{2+}$	pH 7	426 (4.55)	
[(tpm)(phen)Ru(H_2O)]$^{2+}$	pH 7	410 (3.57)	
[(tpm)(4,4′-$(CH_3)_2$-bpy)Ru(H_2O)]$^{2+}$	pH 7	425 (3.87)	

[a] Oxidation of the III,III form by $(NH_4)_2Ce^{IV}(NO_3)_6$.

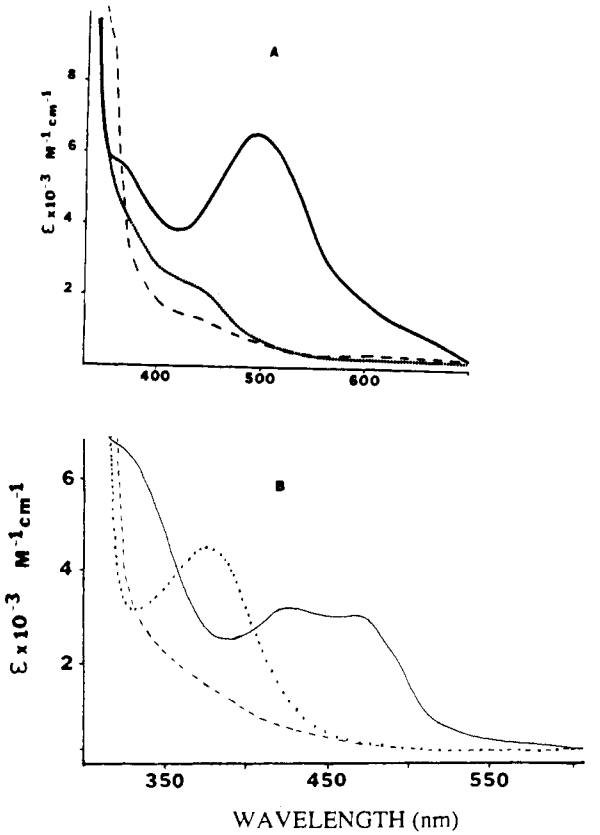

Figure 4. (A) UV–visible spectra at pH 7 of *trans*-[(trpy)(pic)Ru^{II}-(H_2O)]$^+$ (—) and electrochemically generated *trans*-[(trpy)(pic)Ru^{III}-(OH)]$^+$ (···) and *trans*-[(trpy)(pic)Ru^{IV}(O)]$^+$ (- - -). (B) UV–visible spectra of [(tpm)(bpy)Ru^{II}(H_2O)]$^{2+}$ (—) and electrochemically generated [(tpm)(bpy)Ru^{III}(OH)]$^{2+}$ (···) and [(tpm)(bpy)Ru^{IV}(O)]$^{2+}$ (- - -) at pH 7.

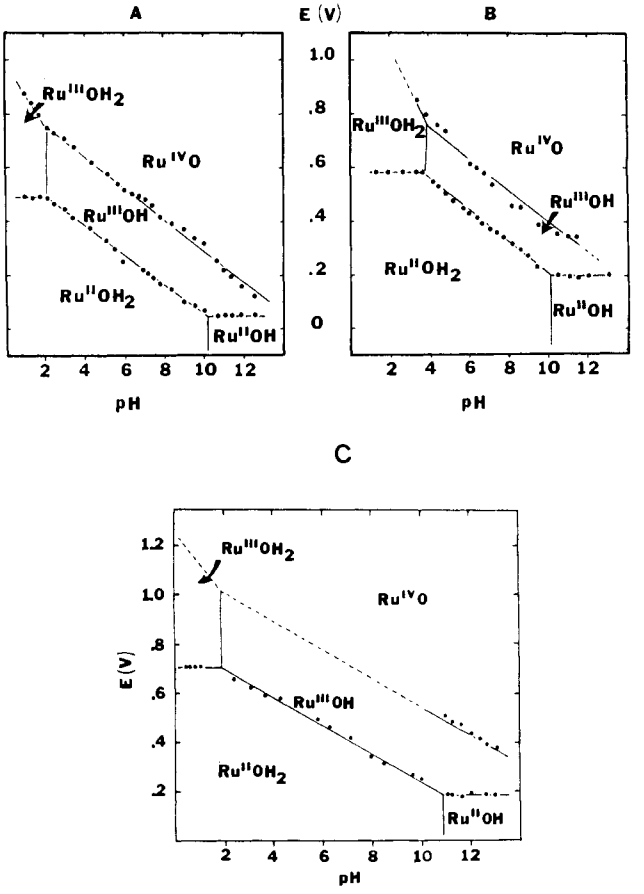

Figure 5. $E_{1/2}$ vs pH or Pourbaix diagram derived from electrochemical measurements on complexes. (A) *trans*-[(trpy)(pic)Ru^{II}(H_2O)]$^+$, (B) *cis*-[(trpy)(pic)Ru^{II}(H_2O)]$^+$ and (C) [(tpm)(bpy)Ru^{II}(H_2O)]$^{2+}$. The pH–potential regions of stability for the various oxidation states and their dominant proton composition are indicated by using abbreviations such as $Ru^{III}OH$, for example, for [(tpm)(bpy)Ru^{III}(OH)]$^{2+}$. The pK_a values are shown by the vertical line in the various E–pH regions.

consistent with a $1H^+$, $2e^-$ process, and the appearance of a 2-electron couple

$$[(trpy)(pic)Ru^{III}—O—Ru^{III}(pic)(trpy)]^{2+} + 2e^- + 1H^+ \longrightarrow [(trpy)(pic)Ru^{II}—(H)O—Ru^{II}(pic)(trpy)]^+ \quad (5)$$

Coulometric reduction (n = 2) of the III,III ions in acidic solution leads to rapid decomposition of the μ-oxo ion and formation of the corresponding monomers. However at pH >11 the twice-reduced dimers are stable, at least for a period of several minutes in solution.

In Figure 4 are shown optical spectra for the various oxidation states of the *trans*-trpy–pic monomer and for the three oxidation states associated with [(tpm)(bpy)Ru(H_2O)]$^{2+}$ at pH 7. λ_{max} values are summarized in Table III for all of the complexes studied here. The spectra for the Ru(III) and Ru(IV) complexes were obtained by coulometric oxidation of the corresponding Ru(II) complexes. Oxidation of *cis*-[(trpy)(pic)Ru(H_2O)]$^+$ leads to the appearance of a low-energy absorption band at λ_{max} = 700 nm characteristic of the μ-oxo ion. The intensity of the band increases with time, and the dimerization process is sufficiently rapid that we have been unable to obtain pure samples of the cis Ru(IV) complex.

The ^1H NMR spectra of the trpy–pic complexes are very complex. However, for [(tpm)(b)Ru(H_2O)](ClO_4)$_2$ (b = bpy, 4,4′-$(CH_3)_2$-bpy) the spectra were assigned (the assignments are listed in the Experimental Section) by taking advantage of the symmetry of the molecules, which leads to an equivalence of two of the three rings of the tpm ligand and simplifies integrations

and coupling constants. In related complexes, coupling constants are known not to vary significantly when the metal, ligand, or solvent are changed.[11]

The chemical shifts for the tpm and bpy protons in $[(tpm)(b)Ru(H_2O)](ClO_4)_2$ appear in regions where expected.[12] The methylenic proton of the tpm ligand is not observed in the spectra due to a fast exchange process with D_2O. Nevertheless, in acetone-d_6 as solvent, a sharp singlet appears at 9.80 ppm, which can be assigned to this proton. Because of the inductive effect of the methyl groups in $[(tpm)(4,4'-(CH_3)_2-bpy)Ru(H_2O)](ClO_4)_2$, the bpy protons are shielded by 0.13–0.15 ppm compared to the bpy complex while the tpm protons remain at the same positions.

Discussion

Redox Properties. Comparisons with Related Monomeric Redox Couples. In the results described here we have added the trpy–pic isomers and the new tpm–bpy systems to the list of aqua/hydroxo/oxo-based Ru(II)/Ru(III)/Ru(IV) couples. The pattern of Ru(III)/Ru(II) and Ru(IV)/Ru(III) couples is entirely analogous to patterns observed earlier, for example for $[(bpy)_2(py)Ru(H_2O)]^{2+}$.[2b] One of the important themes that will hopefully emerge from work of this kind is how ligand variations can be used to tune in a systematic way the redox properties and, through the redox properties, oxidative reactivity.

The most important comparison to be made from the data in Table II is of how the variations in ligands influence potentials for the Ru(III)/Ru(II) and Ru(IV)/Ru(III) couples. Predictably, substitution of the pic ligand for bpy leads to decreases in the potentials for both the Ru(III)/Ru(II) and Ru(IV)/Ru(III) couples. The electronic stereochemical effect associated with the pic ligand appears in the decreased potentials for the *trans*-Ru(III)/Ru(II) and Ru(IV)/Ru(III) couples where the electron-rich carboxylate is trans to the acidic water molecule. For the complexes $[(tpm)(b)Ru(H_2O)]^{2+}$, substitution of 4,4'-bpy for bpy causes a decrease in reduction potentials for both the Ru(VI)/Ru(III) and Ru(III)/Ru(II) couples.

From the first four entries in Table II and, as a general trend, ligand variations in the polypyridyl complexes tend to affect the Ru(III)/Ru(II) couple more strongly than the Ru(IV)/Ru(III) couple. For the $[(bpy)_2(py)Ru(H_2O)]^{2+}$ and $[(trpy)(bpy)Ru(H_2O)]^{2+}$ based couples the potential difference between the Ru(IV)/Ru(III) and Ru(III)/Ru(II) couples is sufficiently small (0.11 and 0.13 V, respectively) that Ru(III) is nearly unstable with respect to disproportionation via, for example

$$2[(bpy)_2(py)Ru^{III}(OH)]^{2+} \rightarrow [(bpy)_2(py)Ru^{II}(H_2O)]^{2+} + [(bpy)_2(py)Ru^{IV}(O)]^{2+} \quad (6)$$

In fact, above pH 12 where a difference in pH dependence exists between the two couples

$$[(bpy)_2(py)Ru^{IV}(O)]^{2+} + e^- + H_2O \rightarrow [(bpy)_2(py)Ru^{III}(OH)]^{2+} + OH^- \quad (7)$$

$$[(bpy)_2(py)Ru^{III}(OH)]^{2+} + e^- \rightarrow [(bpy)_2(py)Ru^{II}(OH)]^{+} \quad (8)$$

Ru(III) does became unstable with respect to disproportionation via

$$OH^- + 2[(bpy)_2(py)Ru^{III}(OH)]^{2+} \rightarrow [(bpy)_2(py)Ru^{IV}(O)]^{2+} + [(bpy)_2(py)Ru^{II}(OH)]^{+} + H_2O \quad (9)$$

One clear inference that can be drawn from the ligand-dependence data is that with the addition of electron-withdrawing substituents which stabilize Ru(II) by $d\pi \rightarrow \pi^*$ back-bonding, it should be possible to increase the Ru(III)/Ru(II) couple relative to the Ru(IV)/Ru(III) couple. By an appropriate manipulation of ligands, it may be possible to create complexes where even at pH 7, $E_{1/2}$(III/II) > $E_{1/2}$(IV/III). In such a coordination environment Ru(III) would be unstable with respect to disproportionation via a reaction like (6) and only the two-electron Ru(IV)/Ru(II) couple would appear in a thermodynamic sense in solution.

Another significant, but opposite, ligand-based effect appears by comparing the facial tpm-based couples with the bis-bpy couples in Table II. The comparison shows that the effect of exchanging a pyrazolyl group in tpm for a pyridyl group in bpy trans to the acidic aqua ligand is to increase the potential of the Ru(III)/Ru(II) couple slightly but the potential of the Ru(IV)/Ru(III) couple is increased by nearly 200 mV. The tpm ligand destablizes the higher oxidation state.

pic-Based μ-Oxo Ions. The pic-based μ-oxo ions are an unavoidable feature of the coordination chemistry of this system and an apparent consequence of the role of stereochemistry at the metal in dictating the ease of μ-oxo ion formation. As is true for $[(bpy)_2(py)Ru^{III}(OH)]^{2+}$, *trans*-$[(trpy)(pic)Ru^{III}(OH)]^{+}$ and the $Ru^{IV}(O)$ complex are stable towards μ-oxo ion formation in water at room temperature. In fact, $[(bpy)_2(py)Ru–O–Ru(py)(bpy)_2]^{4+}$ is a known compound but is unstable toward loss of pyridine at pH 7.[13] The inhibition toward dimer formation of $[(bpy)_2(py)Ru(OH)]^{2+}$ and the trans pic isomer are probably both a consequence of the presence of the sterically demanding pyridine group in the coordination position cis to the Ru–O–Ru bridge (Figure 1A).

A second notable feature in the dimer chemistry is the dramatic difference in the reductive electrochemistry between acetonitrile and water. In water there is a two-electron-reduction process. From the pH-dependence study, a proton is also added, presumably at the oxo group, to form the corresponding μ-hydroxo dimer, reaction 5. Since the reduction process in water is chemically reversible and nearly electrochemically reversible as well, the data show that the intermediate 1-electron mixed-valence Ru(III)–Ru(II) ion is reduced at a potential more positive than the initial reduction and therefore that it is unstable with respect to disproportionation under these conditions, via

$$2[(trpy)(pic)Ru^{III}–O–Ru^{II}(pic)(trpy)]^{+} + H_2O \rightarrow [(trpy)(pic)Ru^{III}–O–Ru^{III}(pic)(trpy)]^{2+} + [(trpy)(pic)Ru^{II}(\mu\text{-}OH)Ru^{II}(pic)(trpy)]^{+} + OH^- \quad (10)$$

By contrast, waves for both the III,III/III,II and III,II/II,II couples are observed in acetonitrile, and the mixed-valence ions are stabilized by 0.6–0.7 V with respect to disproportionation (Table I). The key to the extraordinary difference in behavior in water appears to lie in the availability of protons in water for stabilizing the (II,II) ions by protonation at the μ-oxo bridge to give the μ-hydroxo bridge (reaction 5). Although the potential of the non-proton-involving couples are expected to be somewhat solvent dependent, the dependence is expected to be weak,[15] and $E_{1/2}$ for the III,III/III,II couple in water is not expected to be greatly different from the value of –0.12 V in acetonitrile (Table I). The measured potential in water for the two-electron wave is an average of the potentials for the III,III/III,II and III,II/II,II waves suggesting that, for the 1-electron III,II couple

$$[(trpy)(pic)Ru^{III}–O–Ru^{II}(pic)(trpy)]^{+} + e^- + H^+ \rightarrow [(trpy)(pic)Ru^{II}(\mu\text{-}OH)Ru^{II}(pic)(trpy)]^{+} \quad (11)$$

$E_{1/2} \sim 0.28$ V, in the trans case. The difference between this value and $E_{1/2} = -0.71$ V in acetonitrile for the *trans*-III,II/II,II couple points toward a strongly basic μ-oxo group in the reduced dimer that is greatly stabilized by protonation.

The stabilization of the lower oxidations states of the dimer by protonation is expected on electronic grounds. On the basis of a qualitative MO scheme,[9] addition of electrons to the Ru(I-

(11) Lytle, F. E.; Petrosky, L. M.; Carlson, L. R. *Anal. Chim. Acta* **1971**, *57*, 239.
(12) Pretsch, E.; et al. *Tables of Spectral Data for Structure Determination of Organic Compounds*; Springer-Verlag: West Berlin, 1983; pp H270, H315.
(13) Doppelt, P.; Meyer, T. J. *Inorg. Chem.* **1987**, *26*, 2027.
(14) Diamantis, A. A.; Murphy, W. R.; Meyer, T. J. *Inorg. Chem.* **1984**, *23*, 3230.
(15) (a) Sahami, S.; Weaver, M. J. *J. Electroanal. Chem. Interfacial Electrochem.* **1981**, *122*, 171. (b) Curtis, J. C.; Meyer, T. J.; Hupp, J. T.; Neyhart, G. A., manuscript in preparation.

II)-Ru(III) ions involves π^* levels based on the Ru-O-Ru bridge and the added proton stabilizes the electron-rich Ru-O-Ru group.

Acknowledgments are made to the National Science Foundation under Grant No CHE-8601604 and the National Institutes of Health under Grant No GM32296 for support of this research. A.L. acknowledges fellowship support from Fulbright "La Caixa" (Barcelona, Spain). P.D. acknowledges the Centre Nationale de la Recherche Scientific (CNRS), France, for financial support.

Registry No. *trans*-[(trpy)(pic)RuCl], 111958-91-9; *cis*-[(trpy)(pic)RuCl], 112019-21-3; *trans*-[[(trpy)(pic)Ru]$_2$O](ClO$_4$)$_2$, 111959-06-9; *cis*-[[(trpy)(pic)Ru]$_2$O](ClO$_4$)$_2$, 112019-23-5; [(tmp)(bpy)RuCl]Cl, 111975-11-2; [(tmp)(phen)RuCl]Cl, 111958-92-0; [(tmp)(4,4'-(CH$_3$)$_2$-bpy)RuCl]Cl, 111975-12-3; *trans*-[(trpy)(pic)Ru(H$_2$O)](ClO$_4$), 111959-09-2; *cis*-[(trpy)(pic)Ru(H$_2$O)](ClO$_4$), 112065-87-9; [(tpm)(bpy)Ru(H$_2$O)](ClO$_4$)$_2$, 111958-94-2; [(tpm)(phen)Ru(H$_2$O)](ClO$_4$)$_2$, 111958-96-4; [(tpm)(4,4'-(CH$_3$)$_2$-bpy)Ru(H$_2$O)](ClO$_4$)$_2$, 111958-98-6; *trans*-[(trpy)(pic)Ru(H$_2$O)]$^{3+}$, 111959-10-5; *cis*-[(trpy)(pic)Ru(H$_2$O)]$^{3+}$, 112019-25-7; [(tpm)(bpy)Ru(H$_2$O)]$^{4+}$, 111958-99-7; [(tpm)(phen)Ru(H$_2$O)]$^{4+}$, 111975-13-4; [(tpm)(4,4'-(CH$_3$)$_2$-bpy)Ru(H$_2$O)]$^{4+}$, 111959-00-3; *trans*-[(trpy)(pic)Ru(H$_2$O)]$^{2+}$, 112065-80-2; *cis*-[(trpy)(pic)Ru(H$_2$O)]$^{2+}$, 111959-11-6; [(tpm)(bpy)Ru(H$_2$O)]$^{3+}$, 111959-01-4; [(tpm)(phen)Ru(H$_2$O)]$^{3+}$, 111959-02-5; [(tpm)(4,4'-(CH$_3$)$_2$-bpy)Ru(H$_2$O)]$^{3+}$, 111959-03-6; [(trpy)RuCl$_3$], 72905-30-7; [(tpm)RuCl$_3$], 111975-10-1; *trans*-[(trpy)(pic)Ru^{III}-O-Ru^{IV}(pic)(trpy)]$^{3+}$, 111959-04-7; *cis*-[(trpy)(pic)Ru^{III}-O-Ru^{IV}(pic)(trpy)]$^{3+}$, 112019-24-6; *trans*-[(trpy)(pic)Ru^{II}-OH-Ru^{IV}(pic)(trpy)]$^{+}$, 112065-85-7; *cis*-[(trpy)(pic)-Ru^{II}-OH-Ru^{II}(pic)(trpy)]$^{+}$, 111959-07-0.

Supplementary Material Available: Figure S1 (UV-visible spectra of *cis*-[(trpy)(pic)Ru^{II}(H$_2$O)]$^{+}$ (---) and electrochemically generated *cis*-[(trpy)(pic)Ru^{III}(OH)]$^{+}$ (···) at pH 7), Figure S2 (cyclic voltammograms of (A) *trans*-[(trpy)(pic)Ru^{II}(H$_2$O)](ClO$_4$) at pH 7, (B) *trans*-[(trpy)(pic)Ru^{IV}(O)](ClO$_4$) at pH 3, and (C) *cis*-[(trpy)(pic)Ru^{II}-(H$_2$O)](ClO$_4$) at pH 7 (0.1 M phosphate buffers, scan rate 50 mV/s)), Figure S3 (cyclic voltammograms of *trans*- and *cis*-[[(trpy)(pic)-Ru]$_2$O](ClO$_4$)$_2$ vs SSCE in water at pH 6.5 (0.1 M phosphate buffer, scan rate 50 mV/s)), and Figure S4 (^{1}H NMR spectra of [(tpm)(b)-Ru(H$_2$O)](ClO$_4$)$_2$ in D$_2$O, where (A) b = bpy and (B) b = 4,4'-(CH$_3$)$_2$-bpy) (4 pages). Ordering information is given on any current masthead page.

Contribution from the Department of Chemistry, National Taiwan University, Taipei, Taiwan, Republic of China, and Department of Crystallography and Mineralogy, University of Frankfurt, Frankfurt, West Germany

Experimental Charge Density Study of 1,3-Dithietane 1,1,3,3-Tetraoxide, $(CH_2SO_2)_2$

Yu Wang,*† L. W. Guo,† H. C. Lin,† C. T. Kao,† C. J. Tsai,† and J. W. Bats‡

Received June 1, 1987

A single crystal of 1,3-dithietane 1,1,3,3-tetraoxide, $(CH_2SO_2)_2$, has been studied by X-ray diffraction at 300 and 104 K. It crystallizes in the monoclinic space group $P2_1/n$, with cell parameters a = 5.527 (2) Å, b = 5.709 (2) Å, c = 8.042 (3) Å, and β = 100.89 (3)° at 104 K; Z = 2. The molecule has a four-membered S-C-S-C ring with the center of the ring at $\bar{1}$. There is a short S-S across the ring distance of 2.593 Å. A bonding electron density study was performed with the 104 K data. The X-X deformation map of the four-membered ring shows a significant amount of density around sulfur atom. There is a peak of 0.57 e Å^{-3} in the S-C bond, polarized toward the sulfur atom. The $-SO_2$ and $-CH_2$ planes are nearly perpendicular to the four-membered ring. The accumulation of electron density in the S-O bond is at the center of the bond, comparable with a recent MO calculation. Such comparison led to the experimental proof of the important role of polarization basis sets including d functions of the sulfur atom in the theoretical bonding electron density studies.

Introduction

$(CH_2SO_2)_2$ has been studied by X-ray diffraction at room temperature both in this laboratory and quite independently by Balback et al. in 1980.[1] The crystal is very stable and yields good diffraction intensity measurements. The crystal was chosen to investigate its bonding electron density distribution at low temperature. This molecule is particularly interesting in its small ring structure and its short S-S contact distance. The questions we would like to answer in this study are as follows: First, does the four-membered ring structure suffer from ring strain? Second, is there any contribution in charge density distribution from the d functions of the sulfur atom? Third, what is the character of the S-O bond? Finally, is there any interaction between sulfur atoms across the ring?

Experimental Section

The title compound was prepared by reacting CH_2SO_2Cl with trimethylamine in THF at -20 °C.[2] The suitable colorless single crystals for diffraction studies were obtained by diffusing ethanol into a saturated DMF solution.

The crystal data of $(CH_2SO_2)_2$ at both 300 and 104 K are listed in Table I. The intensity data at both temperatures were collected with CAD4 diffractometer equipped with a graphite monochromator and liquid N_2 gas flow set up. The experimental details are also given in Table I. The intensity data at 104 K were measured up to 2θ of 110°, two (three in some cases) more equivalent reflections were measured up to 86°. Beyond 110°, only 80 calculated strong reflections were measured. These yield a total of 8725 measurements, which gave 3273 unique reflections after averaging of equivalents. A 14% linear decay of

Table I. Crystal Data for $(CH_2SO_2)_2$ at 300 and 104 K

	300 K	104 K
formula	$(CH_2SO_2)_2$	
mol wt	156.17	
cryst size, mm	0.3 × 0.3 × 0.5	0.24 × 0.14 × 0.24
space group	$P2_1/n$	$P2_1/n$
a, Å	5.587 (2)	5.527 (2)
b, Å	5.757 (3)	5.709 (2)
c, Å	8.125 (2)	8.042 (3)
β, deg	100.89 (2)	100.89 (3)
V, Å^3	256.63	249.21
Z	2	2
D_{calcd}, g/cm^3	2.021	2.081
F_{000}	160	160
radiation	Mo Kα (λ = 0.7107 Å)	Mo Kα
scan speed, deg/min	20/3	20/3-20/16
2θ range (Mo Kα), deg	4-54	5-128.1
$\theta/2\theta$ scan param	2(1.0 + 0.35 tan θ)	2(0.95 + 0.5 tan θ)
abs coeff, cm^{-1}	9.4	9.4
transmittance factor		0.79-0.89
total no. of reflcns	682	3273
no. of obsd rflcns (>2σ)	494	3068
$\sum_i I_i - \langle I \rangle / \sum_i I_i$		0.013
quadrant collcd	$h,k,\pm l$	$h,k,\pm l$; $h,-k,\pm l$; additional $-h,\mp k,\pm l$
R, R_w	0.033, 0.028	0.030, 0.027
S	2.43	1.51
f ($W(f) = 1/[\sigma_c^2(F_o) + fF_o^2]$)	0	0.000 07

* To whom correspondence should be addressed.
† National Taiwan University.
‡ University of Frankfurt.

